

## Large-Scale Monte Carlo Study of a Realistic Lattice Model for $\text{Ga}_{1-x}\text{Mn}_x\text{As}$

Yucel Yildirim,<sup>1,2</sup> Gonzalo Alvarez,<sup>3</sup> Adriana Moreo,<sup>1</sup> and Elbio Dagotto<sup>1</sup>

<sup>1</sup>*Department of Physics and Astronomy, University of Tennessee, Knoxville, Tennessee 37966-1200, USA  
and Oak Ridge National Laboratory, Oak Ridge, Tennessee 37831-6032, USA*

<sup>2</sup>*Department of Physics, Florida State University, Tallahassee, Florida 32306, USA*

<sup>3</sup>*Computer Science and Mathematics Division and Center for Nanophase Materials Sciences, Oak Ridge National Laboratory,  
Oak Ridge, Tennessee 37831-6032, USA*

(Received 30 November 2006; revised manuscript received 9 February 2007; published 1 August 2007)

Mn-doped GaAs is studied with a real-space Hamiltonian on an fcc lattice that reproduces the valence bands of undoped GaAs. Large-scale Monte Carlo (MC) simulations on a Cray XT3, using up to a thousand nodes, were needed. Spin-orbit interaction and the random distribution of the Mn ions are considered. The hopping amplitudes are functions of the GaAs Luttinger parameters. At the realistic coupling  $J \sim 1.2$  eV the MC Curie temperature and magnetization curves agree with experiments for  $x = 8.5\%$  annealed samples. Mn-doped GaSb and GaP are also briefly discussed.

DOI: 10.1103/PhysRevLett.99.057207

PACS numbers: 75.50.Pp, 71.10.Fd, 72.25.Dc

*Introduction.*—The study of diluted magnetic semiconductors (DMS) is a rapidly expanding area of research [1–3] triggered by the discovery of high Curie temperatures ( $T_C$ ) in some of these materials, and by their potential role in spintronics devices [4]. Experimentally, much progress in the study of DMS was recently achieved after annealing techniques reduced the rates of compensation, allowing for higher  $T_C$ 's and for the intrinsic properties of DMS materials to be carefully investigated [5]. Theoretical studies of DMS have focused on two idealized scenarios: (1) impurity-band (IB) models [6], and (2) hole-fluid (HF) models (based on mean-field approximations) [2,7]. These two models lead to dramatically different predictions of many physical quantities in DMS, such as in the behavior of the magnetization with temperature and in the contribution of an impurity band to their physical properties. Since experimental evidence for both scenarios has been reported in similar ranges of doping and compensation [5,8], the issue of the correct intrinsic behavior and microscopic description of DMS is still open.

The rather different theoretical views of the same problem presented by IB and HF models, and the fact that real DMS systems are likely to have coupling constants and carrier densities that are between the extreme values assumed by these models, suggests a need for flexible theoretical methods that can interpolate between these model limits using the same formalism. However, while considerable progress has been achieved in numerical studies of simplified models [9], the complexity of the real problem (involving several bands on an fcc lattice) has prevented its detailed analysis until now.

Here, we report a comprehensive numerical Monte Carlo study of a multiband lattice model for Mn-doped GaAs, including spin-orbit (SO) coupling, as well as the effects of random Mn doping. This study would have taken several years without access to a supercomputer with thousands of processors, such as the Cray XT3.

*The model.*—We have constructed a real-space fcc-lattice Hamiltonian whose kinetic-energy term maps into the Luttinger-Kohn model [10] when the Hamiltonian is Fourier transformed and the limit  $k \rightarrow 0$  is taken. Then, the hopping amplitudes are precisely known since they are functions of (tabulated) Luttinger parameters (LP) [11]. To incorporate the SO interaction, we work in the  $|j, m_j\rangle$  basis, where  $j$  can be  $3/2$  or  $1/2$  (considering the  $p$  orbitals,  $l = 1$ , relevant at the  $\Gamma$  point of the GaAs valence band). Since there are 6 possible values for  $m_j$ , this is a fully 6-orbital approach, arising from the 3 original  $p$  orbitals and the 2 hole spin projections. The Hamiltonian is

$$H = \frac{1}{2} \sum_{\mathbf{i}, \mu, \nu, \alpha, \alpha', a, b} (t_{\alpha a, \alpha' b}^{\mu \nu} c_{\mathbf{i}, \alpha a}^\dagger c_{\mathbf{i} + \boldsymbol{\mu} + \boldsymbol{\nu}, \alpha' b} + \text{H.c.}) + \Delta_{\text{SO}} \sum_{\mathbf{i}, \alpha} c_{\mathbf{i}, \alpha \frac{1}{2}}^\dagger c_{\mathbf{i}, \alpha \frac{3}{2}} + J \sum_{\mathbf{I}} \mathbf{s}_{\mathbf{I}} \cdot \mathbf{S}_{\mathbf{I}}, \quad (1)$$

where  $a, b$  take the values  $\frac{1}{2}, \frac{3}{2}$  (for  $j = 3/2$ ), or  $\frac{1}{2}$  (for  $j = 1/2$ ), and  $\alpha$  and  $\alpha'$  can be 1 or  $-1$ . The Hund term describes the interaction between the hole spins  $\mathbf{s}_{\mathbf{I}}$  and the spin of the localized Mn ion  $\mathbf{S}_{\mathbf{I}}$ . The latter is considered classical ( $|\mathbf{S}_{\mathbf{I}}| = 1$ ) [12], since it is large  $S = 5/2$  [13].  $\boldsymbol{\mu} + \boldsymbol{\nu}$  are the 12 vectors indicating the 12 nearest-neighbor sites of each ion located at site  $\mathbf{i}$ , while  $\mathbf{I}$  are random sites in the fcc lattice.  $\Delta_{\text{SO}} = 0.341$  eV is the SO interaction strength [14] in GaAs. The hopping parameters,  $t_{\alpha a, \alpha' b}^{\mu \nu}$ , are complex numbers, functions of the LP [15].

Equation (1) can be studied with standard Monte Carlo (MC) techniques for systems involving fermions and classical spins [9,16]. Numerically, we analyze clusters that contain  $N = N_x N_y N_z$  unit cells ( $N_i$  is the number of cells along the spatial direction  $i$ ) of side  $a_0$  ( $a_0 = 5.64$  Å [14], is the GaAs cubic lattice parameter). Since in an fcc lattice there are 4 ions per unit cell, the total number of Ga sites is  $N_{\text{Ga}} = 4N$ . Since there are 6 single fermionic states per

site, the diagonalization of a  $6N_{\text{Ga}} \times 6N_{\text{Ga}}$  matrix is needed at each step of the MC simulation, which demands considerable computational resources. The diagonalization can be performed exactly for values of  $N_{\text{Ga}}$  up to 500. Lattices with  $N_i = 4$  (256 sites) are adequate to study Mn dopings  $x$  and relative hole densities  $p$  in the range of interest, with sufficient precision for our purposes. Nominally there should be one hole per Mn ion, but  $p$  can be smaller than 1 due to hole trapping defects; thus,  $p$  and  $x$  are here considered independent.

**Results.**—The highest  $T_C$  experimentally observed in  $\text{Ga}_{1-x}\text{Mn}_x\text{As}$  is 173 K for  $x = 9.0\%$  and a  $p$  believed to be close to 1 [17]. For known values of  $x$  and  $p$ , the highest reported  $T_C$  is  $\sim 150$  K at  $x = 8.5\%$  and  $p \approx 0.7$  [17,18]. The system is metallic, and the magnetization vs temperature displays MF behavior [18]. In Fig. 1(a), we present the (MC calculated)  $T_C$  as a function of the coupling  $J$ , at  $x = 8.5\%$  and  $p \approx 0.75$ . Results were obtained on lattices containing 256 (Ga,Mn) ions, and averaging over at least 5 different disorder configurations. Results for lattices with up to 500 sites were calculated for some parameters (see below). At the realistic  $J = 1.2$  eV [19], Fig. 1(a) shows that the critical temperature is  $T_C = 155 \pm 20$  K. Since  $J$  is not accurately known, this good agreement with experiment [18] is partially fortuitous, but at least the results indicate that a reasonable estimation of the real  $T_C$  can be made via MC simulations of lattice models. The solid line in the figure corresponds to the mean-field (MF) results [2,20,21]. The quantitative MF-MC agreement at small  $J$  provides a strong test of the present MC approach. At  $J = 1.2$  eV, the MF  $T_C$  is  $\sim 300$  K, showing that at these

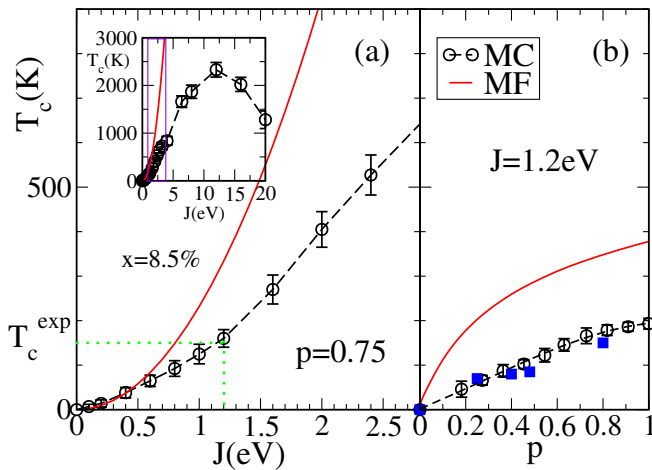


FIG. 1 (color online). (a) Calculated  $T_C$  vs  $J$  for (Ga,Mn)As with  $x = 8.5\%$  and relative hole density  $p \approx 0.75$ . Circles are the MC results, the continuous line is the MF prediction [2,20,21]. Inset: MC results for larger values of  $J$  to observe the crossover toward a localized picture. Vertical lines indicate the experimentally acceptable range of  $J$ . (b) MC calculated  $T_C$  vs  $p$ , at  $x = 8.5\%$ . The blue dots are experimental results [18], and the solid line is the MF prediction.

couplings and densities appreciable differences between MC calculations and MF exists: the fluctuations considered in the MC approach cannot be neglected. The inset of Fig. 1 demonstrates that for  $J \gtrsim 0.5$  eV, the MF approximation breaks down [22].

At  $J \sim 1.2$  eV,  $x = 0.085$  and  $p \sim 0.75$  the (Ga,Mn)As system is closer to a hole-fluid than a localized regime as suggested by the  $M$  vs  $T$  curve [Fig. 2(a)]. This curve has a Curie-Weiss (CW) shape, in qualitative agreement with both experimental results [18] and previous MF calculations [7,20,21]. Size effects are mild, as can be seen in Fig. 3(a) where data for  $M$  vs  $T$  are presented for  $x = 8.5\%$ ,  $p \approx 0.75$ , and  $J = 1.2$  eV, using lattices with  $(N_x, N_y, N_z) = (4, 3, 3)$ ,  $(4, 4, 4)$ ,  $(5, 4, 4)$ , and  $(6, 4, 4)$ , i.e., with  $N_{\text{Ga}} = 144, 256, 320$ , and  $384$ . Results for  $N_{\text{Ga}} = 500$  were obtained for lower doping [see Fig. 2(b)]. Considering together the results for the different size clusters the estimated  $T_C \approx 155 \pm 15$  K is still in agreement with experiments (and also with the 256 sites results). Although a more detailed scaling analysis is needed to confirm our conclusions, at present there is no obvious evidence of strong size effects in our data.

Regarding the CW shape of the magnetization curve, we have phenomenologically observed that the finite SO coupling plays an important role in this respect. In Fig. 3(b) we show the calculated  $M$  vs  $T$  for (Ga,Mn)As with  $x = 8.5\%$ ,  $p = 0.75$ , and  $J = 1.2$  eV for  $\Delta_{\text{SO}} = 0.34$  eV (squares) and  $\Delta_{\text{SO}} = 0$  (circles): only the nonzero SO coupling produces CW behavior. We have noticed that the CW

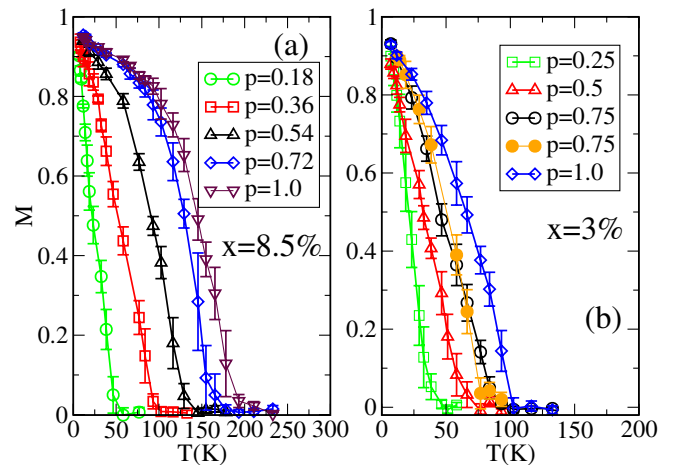


FIG. 2 (color online). (a) Calculated magnetization  $M$  vs  $T$ , for (Ga,Mn)As with  $x = 8.5\%$  and several values of  $p$  (indicated), using a 256 sites lattice (open symbols). Averages over 5 Mn-disorder configurations are shown. (b) Same as (a), but for  $x = 3\%$ . Close circles are results for a 500 sites lattice. The magnetization is measured as  $\mathcal{M} = \sqrt{\mathbf{M} \cdot \mathbf{M}}$ , with  $\mathbf{M}$  the vectorial magnetization. As a consequence, for fully disordered spins,  $\mathcal{M}$  is still nonzero due to the  $\mathbf{S}_i^2 = 1$  contributions, causing a finite value at large temperatures ( $\mathcal{M}(T \rightarrow \infty) = 1/\sqrt{xN_{\text{Ga}}}$ ) unrelated to ferromagnetism. Thus, we plotted  $M = [\mathcal{M} - \mathcal{M}(T \rightarrow \infty)]/[1 - \mathcal{M}(T \rightarrow \infty)]$ ; i.e., the background was subtracted.

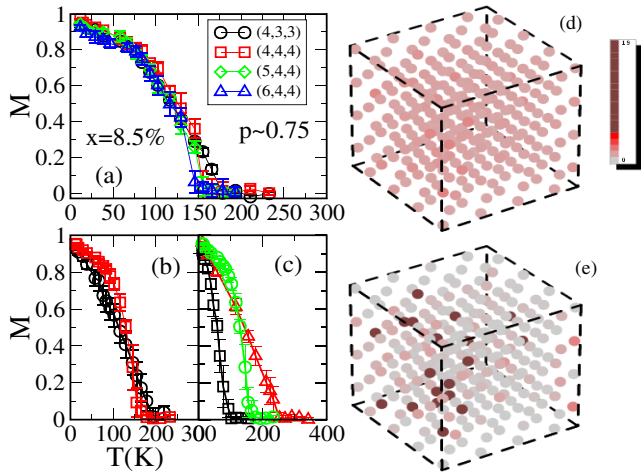


FIG. 3 (color online). (a) Calculated  $M$  (see Fig. 2) vs  $T$  for (Ga,Mn)As for different lattice sizes with  $x = 8.5\%$ ,  $p \approx 0.75$ , and  $J = 1.2$  eV; (b) Calculated  $M$  vs  $T$  for (Ga,Mn)As for the same parameters as in (a) on a 256 sites lattice with (without) SO interaction indicated by the squares (circles); (c)  $M$  vs  $T$  for Mn-doped GaSb (squares), GaAs (circles), and GaP (triangles) for the same parameters as in (b); the respective values of  $\Delta_{SO}$  are 0.76, 0.34, and 0.08 eV; (d) Charge density in (Ga,Mn)As normalized to the MF value (see text), for  $x = 8.5\%$ ,  $p \approx 0.75$ ,  $T = 10$  K, on a 256-sites cluster for  $J = 1.2$  eV. Color intensity is proportional to the charge density (see scale). (e) Same as (d), but for  $J = 12$  eV.

shape is also missing with the 4 orbital (with  $j = 3/2$ ) model that results in the limit  $\Delta_{SO} \rightarrow \infty$  [15]. This indicates the important role that a multiband representation of the valence band (VB) plays in properly describing the thermodynamic observables. The  $M$  vs  $T$  for Mn-doped GaSb and GaP displayed in Fig. 3(c) also support this observation. In the high  $p$  regime for (Ga,Mn)Sb with  $\Delta_{SO} = 0.75$  eV, CW behavior is observed, while in (Ga,Mn)P with  $\Delta_{SO} = 0.08$  eV it is not. The curves have been obtained using Eq. (1) [23]. Notice that the  $T_C = 80$  K (260 K) for GaSb (GaP) is in qualitative agreement with other predictions in the literature [2]. Experimental studies of (Ga,Mn)P are at an early stage, and the compensation rate and ionic state of the Mn are not well known [24]. The current model would (would not) describe (Ga,Mn)P if  $Mn^{2+}$  ( $Mn^{3+}$ ) were present.

In the HF scenario, the charge is assumed to be uniformly distributed, while in the IB picture, the charge is strongly localized. Figure 3(d) indicates that in the high- $T_C$  experimental regime with  $J = 1.2$  eV,  $x = 8.5\%$ , and  $p \approx 0.75$ , the charge is fairly uniformly distributed. The slightly darker points correspond to the sites where the Mn are located. They have charge of the order of 20% above the MF value defined as  $n_{MF} = n/N_{Ga}$  (with  $n$  the number of holes). As shown in Fig. 3(e), charge localization occurs when  $J$  is increased to large values such as 12 eV. The dark circles at the Mn sites have charge intensities about

20 times the MF value, with very little charge found away from the impurities.

The lack of charge localization effects in the ordered state of (Ga,Mn)As is associated with the absence of an impurity band in the density of states (DOS) [Fig. 4(a)]. However, increasing  $J$ , an IB regime is eventually observed, giving confidence that the study is truly unbiased. This occurs for  $J \approx 4$  eV and beyond, with the IB becoming detached from the VB at  $J \approx 16$  eV. Figures 3(d), 3(e), and 4(a) show that the degree of hole localization is correlated with the development of the IB. In addition, when the holes are localized, the  $M$  vs  $T$  curves have substantial deviations from MF behavior (not shown), with a different concavity as in Fig. 2(a) [9].

It is known that the carrier density in DMS is strongly dependent on sample preparation. Because of defects,  $p$  is smaller than 1 in most samples. In Fig. 1(b), the MC calculated  $T_C$  vs  $p$  for (Ga,Mn)As with  $x = 8.5\%$  and  $J = 1.2$  eV is shown.  $T_C$  increases with  $p$ , and it reaches a maximum at  $p \sim 1$  as in previous theoretical [2,9] and experimental results [5,18,25,26]; an example of the latter is also included in Fig. 1(b). The MC experiments agreement is once again satisfactory. The figure suggests that if  $p = 1$  were reachable experimentally,  $T_C$  could be as high as  $\sim 200$  K. We also observed qualitative changes in the magnetization curves as  $p$  varies [Fig. 2(a)]: as  $p$  is reduced,  $M$  changes from a Brillouin form to an approximately linear shape with  $T$ . This observed  $p$  dependence is similar to the experimental results, in which  $p$  is modified by annealing [18]; Mn disorder plays a more dominant role when the number of holes is reduced.

Consider now the low Mn-doping regime. The latest experimental results suggest that (Mn,Ga)As should still be metallic at  $x = 3\%$  [25]. A metal-insulator transition (MIT) is expected at  $x \leq 1\%$  [27], but MC studies for such very small dopings need much larger clusters than cur-

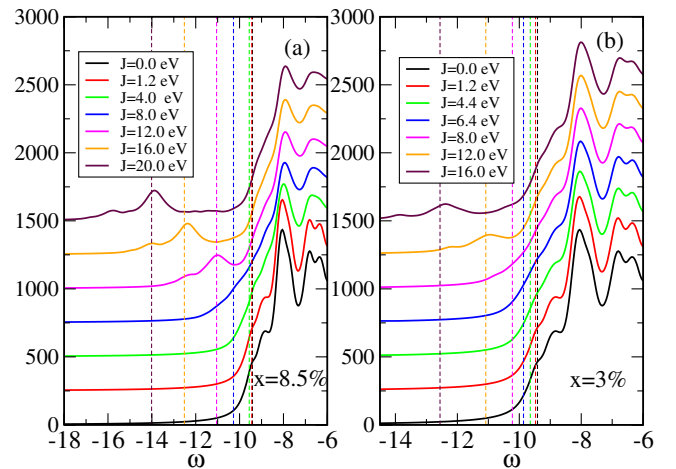


FIG. 4 (color online). (a) MC density-of-states for (Ga,Mn)As with  $x = 8.5\%$ ,  $p \approx 0.75$ , and several  $J$ 's. Dashed lines indicate chemical potentials. (b) Same as (a) but for  $x = 3\%$ .

rently possible [28]. Our MC simulations indicate that at the lowest Mn-doping studied here, the dependence of  $T_C$  with  $J$  is similar to that observed at higher doping. No clearly formed IB is observed in the  $x = 3\%$  DOS displayed in Fig. 4(b) at  $J = 1.2$  eV. However, the IB's are formed with increasing  $J$ , at both  $x = 3\%$  and  $8.5\%$ , as deduced from an analysis of fermionic eigenvalues for spin-ordered configurations [15,29]. Intuitively, it is expected that the IB scenario should be valid at sufficiently small  $x$  and  $p$ , outside the range of this effort.

*Summary.*—Here, a MC study of an fcc-lattice model for DMS compounds, including the many VB of GaAs, the SO interaction, and the random distribution of Mn dopants, has been presented. The results show magnetizations and  $T_C$ 's in reasonable agreement with experiments. The simulations show that the carriers tend to spread over the entire lattice at  $x = 0.085$ , and they reside in the VB, qualitatively in agreement with MF [2,7] and first principles [3] calculations in the same parameter regime, as well as with experimental data on annealed samples [5,25]. However, an IB band populated by a fraction  $1-p$  of trapped holes that do not participate in the transport properties is not ruled out by our results. The IB scenario should be valid at sufficiently small  $x$  and  $p$ . This MC method opens a new semiquantitative window for theoretical research on DMS materials.

We acknowledge discussions with T. Dietl, A. MacDonald, J. Sinova, T. Schulthess, F. Popescu, and J. Moreno. Y. Y., A. M., and E. D. are supported by NSF under Grants No. DMR-0443144 and No. DMR-0454504. This research used resources of the NCCS. G. A. is sponsored by the Division of Scientific User Facilities, BES, DOE, Contract No. DE-AC05-00OR22725 with ORNL, managed by UT-Battelle.

- 
- [1] T. Jungwirth *et al.*, Rev. Mod. Phys. **78**, 809 (2006).
  - [2] T. Dietl *et al.*, Science **287**, 1019 (2000).
  - [3] T. Schulthess *et al.*, Nat. Mater. **4**, 838 (2005).
  - [4] I. Zutic *et al.*, Rev. Mod. Phys. **76**, 323 (2004).
  - [5] S. J. Potashnik *et al.*, Appl. Phys. Lett. **79**, 1495 (2001).
  - [6] M. Berciu and R. Bhatt, Phys. Rev. Lett. **87**, 107203 (2001); H. Akai, Phys. Rev. Lett. **81**, 3002 (1998).
  - [7] M. Abolfath *et al.*, Phys. Rev. B **63**, 054418 (2001).
  - [8] K. S. Burch *et al.*, Phys. Rev. Lett. **97**, 087208 (2006).
  - [9] One-band models (fermions exactly diagonalized) were studied in G. Alvarez *et al.*, Phys. Rev. Lett. **89**, 277202 (2002); M. Mayr *et al.*, Phys. Rev. B **65**, 241202 (2002); See also M. Calderón *et al.*, Phys. Rev. B **66**, 075218 (2002); M. Kennett *et al.*, Phys. Rev. B **66**, 045207 (2002); S. Das Sarma *et al.*, Phys. Rev. B **67**, 155201 (2003);

- J. Schliemann *et al.*, Phys. Rev. B **64**, 165201 (2001); J. Xu *et al.*, Phys. Rev. Lett. **94**, 097201 (2005); F. Popescu *et al.*, Phys. Rev. B **73**, 075206 (2006).
- [10] J. M. Luttinger and W. Kohn, Phys. Rev. **97**, 869 (1955).
- [11] J. M. Luttinger, Phys. Rev. **102**, 1030 (1956). The hoppings here are of order 1 eV. We assumed that they are not affected by the Mn doping, consistent with ARPES measurements: J. Okabayashi *et al.*, Phys. Rev. B **64**, 125304 (2001); Physica (Amsterdam) **10E**, 192 (2001).
- [12] The classical limit corresponds to  $\lim_{\hbar \rightarrow 0, S \rightarrow \infty} \hbar S = \hbar_0 = 6.58 \times 10^{-16}$  eV s. Since the parameter  $J$ , experimentally measured, is proportional to  $\hbar$  via the Bohr magneton, it results that  $J = K\hbar$ , where  $K$  is a constant. Thus,  $\lim_{\hbar \rightarrow 0, S \rightarrow \infty} JS = \lim_{\hbar \rightarrow 0, S \rightarrow \infty} K\hbar S = K\hbar_0 = J$ . See G. Q. Pellegrino *et al.*, Chaos **5**, 463 (1995); G. Q. Pellegrino *et al.*, Revista Brasileira de Ensino de Fisica **20**, 321 (1998); L. G. Yaffe, Rev. Mod. Phys. **54**, 407 (1982).
- [13] J. Szczytko *et al.*, Phys. Rev. B **60**, 8304 (1999); M. Linnarsson *et al.*, Phys. Rev. B **55**, 6938 (1997).
- [14] Peter Yu and Manuel Cardona, *Fundamentals of Semiconductors* (Springer-Verlag, Berlin, 2005), 3rd ed.
- [15] Details will be published elsewhere.
- [16] E. Dagotto *et al.*, Phys. Rep. **344**, 1 (2001).
- [17] T. Jungwirth *et al.*, Phys. Rev. B **72**, 165204 (2005); K. Y. Wang *et al.*, AIP Conf. Proc. **772**, 333 (2005).
- [18] K. C. Ku *et al.*, Appl. Phys. Lett. **82**, 2302 (2003).
- [19] J. Okabayashi *et al.*, Phys. Rev. B **58**, R4211 (1998).
- [20] T. Dietl (private communication).
- [21] T. Dietl *et al.*, Phys. Rev. B **63**, 195205 (2001).
- [22] The MC simulations show that  $T_C$  reaches a maximum for  $J \approx 12$  eV, of the order of the carriers bandwidth, and then it decreases due to hole localization [9].
- [23] The hoppings in each case are obtained from the LP and  $J$  following Ref. [2], which gives  $J_{\text{GaSb}} = 0.64$  eV and  $J_{\text{GaP}} = 1.34$  eV.  $\Delta_{\text{SO}}$ 's are taken from Ref. [14].  $p = 0.75$  has been chosen since CW behavior is expected only for low compensation.
- [24] N. Theodoropoulou *et al.*, Phys. Rev. Lett. **89**, 107203 (2002); M. Scarpulla *et al.*, *ibid.* **95**, 207204 (2005).
- [25] K. W. Edmonds *et al.*, Appl. Phys. Lett. **81**, 3010 (2002).
- [26] S. J. Potashnik *et al.*, Phys. Rev. B **66**, 012408 (2002).
- [27] S. Yang and A. MacDonald, Phys. Rev. B **67**, 155202 (2003).
- [28] According to Mott's criterion [M. Berciu and R. Bhatt, Phys. Rev. B **69**, 045202 (2004)] a MIT should occur when  $(n_c)^{1/3} a_B \sim 0.25$ . In our case  $n_c = 4px/a^3$  (critical concentration) and  $a_B = 8 \text{ \AA}$  (effective Bohr radius). Thus, the MIT should occur for  $px \approx 0.001$ , smaller than the values of  $px$  that we can access. Thus, we are always in the metallic region. The criterion may not be valid for arbitrary  $J$ .
- [29] For the effect of an attractive Coulomb interaction see F. Popescu *et al.*, arXiv:cond-mat/07050309 [Phys. Rev. B (to be published)].